A Statistical Dominance Algorithm for Edge Detection and Segmentation of Medical Images

Adam Piórkowski[1]

Department of Geoinfomatics and Applied Computer Science
AGH University of Science and Technology,
A. Mickiewicza 30 Av., 30–059 Cracow, Poland
pioro@agh.edu.pl

Abstract. This article proposes an algorithm which performs the initial stage of edge detection or segmentation. The algorithm counts the number of pixels with a given relation to the central point of the neighborhood. The output image is a statistical result of the dominance of points over their neighborhoods and allows the classification of these points to be determined (peak, valley, and slope). Therefore, this solution allows the impact of noise or uneven illumination in image results to be reduced.
The basic features of the proposed algorithm are considered in this paper. Application of the algorithm is illustrated in the context of image segmentation of a corneal endothelium with a specular microscope, images of specimens of the brain tissue, and hand radiographs[1].

Keywords: edge detection, segmentation, cell counting, image processing, preprocessing, microscopy images

1 Introduction

The analysis of medical images requires appropriate data preprocessing and ends with binarisation and/or segmentation. The aim is to analyze the location, size or shape of objects by extracting them in binary form or in the form of their boundaries. The diversity of data often does not allow the use of well-known algorithms to set parameters without an adaptive approach. Binarization methods used, such as the one proposed by Otsu [16], or Top-Hat and edge detection used by Prewitt, Sobel or Canny [5] does not always yield the required results. In this article a new method is proposed that effectively performs the binarization or supports segmentation of a fairly large class of images.

2 Statistical Dominance Algorithm

This algorithm was established initially in a 3x3 version as a neighborhood map for multi-stage image thinning after binarization (application: corneal endothelium) [19]. The presented approach makes a segmentation repeatable, objective,

[1] Piorkowski A.: A Statistical Dominance Algorithm for Edge Detection and Segmentation of Medical Images. AISC vol. 471, Springer 2016, pp. 3-14.

and unambiguous. Research has shown that simply making a 'neighborhood map' provides very interesting results for binarization of grayscale images. The most similar algorithm was presented in [24], but it considers fixed levels which are not dependent on neighboring pixels. The Local Binary Patterns algorithm is also related to the algorithm presented here in that it counts the sign of the differences between the central pixel value and its neighbors pixel values, sampled on a circle of given radius [14, 22]. A related issue is also mentioned in geospatial processing, where counting filters are used to count the number of point features, such as houses, wells or landslides [1].

2.1 The Main Idea

The basic idea of the algorithm is to determine for each pixel the number of neighbors in an area with a radius R. The resulting value is the number of pixels whose brightness is greater than or equal to the brightness of the central pixel. The output image is a statistical result of the dominance of points over their neighborhoods and allows the classification of these points to be determined (peak, valley, and slope).

2.2 Options of the Algorithm

The algorithm has the following options:

- two relationships between the central point and points in the neighborhood with equal or greater brightness (>= or >); other relationships (< or <=) which correspond to the first two relations for inverted images,
- additional threshold of the relationship (especially useful for noisy images, e.g. 1-2% of dynamic range),
- neighborhood reduced to a straight line. A directional version of algorithm with lower computational complexity.

In general cases, assuming any shape and size of the relevant neighborhood, the algorithm is similar to formula 1. Equation 2 represents a constructive approach to the round neighborhood (disc) with a specified radius.

$$p\prime(x,y) = \sum_{p_b \in B(x,y)} \begin{cases} p'(x,y) := p'(x,y) + 1, & p_b(x_b, y_b) \geq p(x,y) + t \\ p'(x,y) := p'(x,y), & \text{otherwise} \end{cases} \tag{1}$$

$$p\prime(x,y) = \sum_{i=-N,j=-N}^{i=N,j=N} \begin{cases} p'(x,y) := p'(x,y) + 1, & p(x+i, y+j) \geq p(x,y) + t, \\ & i^2 + j^2 \leq R^2 \\ p'(x,y) := p'(x,y), & \text{otherwise} \end{cases} \tag{2}$$

where:

- $p(x,y)$ - the value of pixel (x,y) in input image,

- $p'(x, y)$ - the value of pixel (x, y) in output image,
- $B(x, y)$ - a neighborhood of pixel $p(x, y)$,
- $p_b(x_b, y_b)$ - the value of p_b pixel of $B(x, y)$ neighborhood (input image),
- R - radius of neighborhood,
- N - size of neighborhood mask, $N = \lceil R \rceil$
- t - *threshold* - the optional difference to be checked.

2.3 The Code

The Statistic Dominance Algorithm

```
for (x = N; x < SX - N; x++)
  for (y = N; y < SY - N; y++)
  {
    imgout[x,y] = 0; // initialization

    for (i = -N; i <= N; i++)
      for (j = -N; j <= N; j++)
        if (i * i + j * j <= R * R)  //without calling sqrt()
          if (imgin[x + i, y + j] >= imgin[x, y] + threshold)
            imgout[x, y]++;
  }
```

where:

- *imgin* - input image,
- *imgout* - output image,
- SX, SY - width and height of input/output image,
- R - (floating point) radius of neighborhood,
- N - (integer) size of neighborhood mask (also size of mirror margin, not presented here), $N = \lceil R \rceil$
- *threshold* - t - the optional difference to be checked (especially for noisy images).

2.4 Features of the Algorithm

The features of the algorithm are:

- the algorithm is designed for grayscale images,
- the result depends on the objects contained in the image, the selection of the size of radius R is therefore a function of the expected object size,
- the range of values in the output image is strictly defined (maximum value is the number of pixels at radius R),
- the result is mostly independent of differences in the brightness of objects in different areas of a picture as only the selected relation is taken into account, so it is easy to process images with varying levels of signal and noise and with local distortions.

As an example showing the last feature mentioned above an analysis of the two profiles could be provided (directional version assumed for simplicity) that have the same course (but not values) of valleys and peaks, thereby producing the same output from the algorithm (Fig. 1).

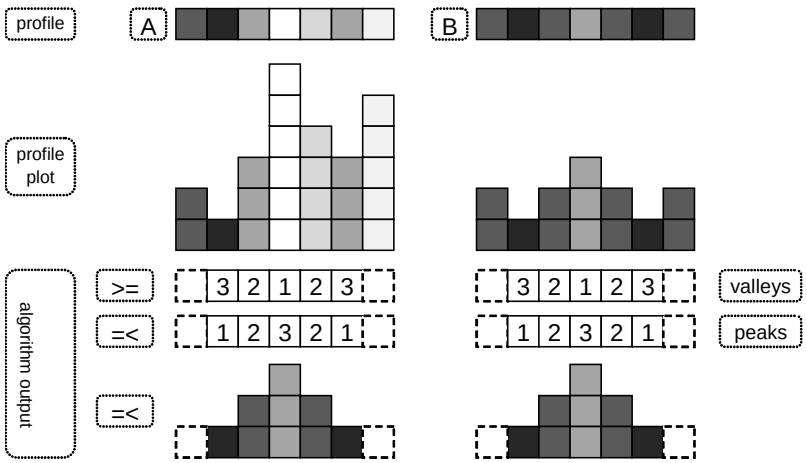

Fig. 1. An example: two profiles with the same course of valleys and peaks but different values, R=1.

3 Examples

3.1 Corneal Endothelium Images from Specular Microscopy

Corneal endothelium images obtained from specular/confocal microscopy are very difficult to preprocess and analyse. There have been a few attempts to carry out proper segmentation, but all of them needed manual correction. Watershed algorithms seem to be useless. The most promising method, which considers a stochastic approach to segmentation, is presented in [20]. An interesting approach of active contour use is presented in [6].

An example of a corneal endothelium image is shown in Fig. 2. The original input (Fig. 2(a), normalized) contains a clear distinction between cells on the right side, and blurred boundaries between shapes on the left side. The SDA algorithm makes it possible to highlight the appropriate boundaries in both sides. Fig. 2(b) contains SDA output after preprocessing with smoothing and a maximal filter (3×3), and Fig. 2(d) shows the same combination for a bigger radius (3). The boundaries are clear. Fig. 2(c) contains the same case as Fig. 2(b), but without a maximal filter. Pure output of the SDA algorithm without any preprocessing, for big radius ($R = 9$), is shown in Fig. 2(e), which also allows highlighting of cell boundaries. The final SDA outputs in Fig. 2 are inverted for printing purposes.

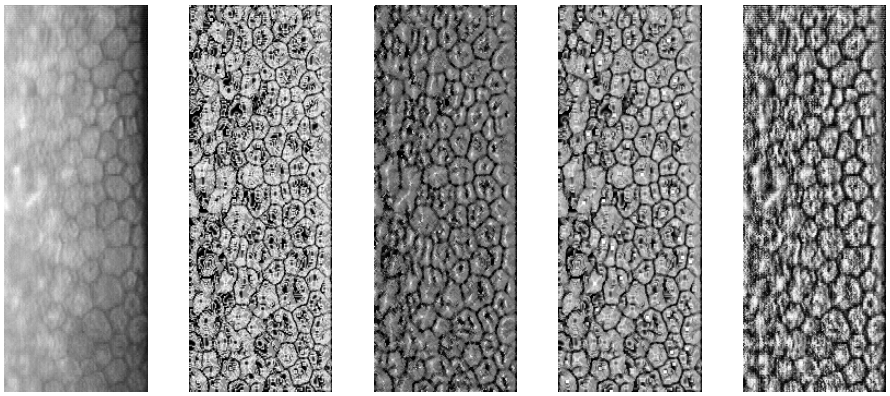

(a) original, normalized (b) max, SDA, R=2 (c) SDA, r=3 (d) max, SDA, R=3 (e) SDA, R=9, no preproc

Fig. 2. Corneal endothelium image processing examples

3.2 Microscopic Images of the Brain Sections

Cell counting is a standard procedure of microscopic image analysis [11]. The aim is to count all cells in the selected region of interest (ROI), for example, a sagittal section of the molecular layer in the cerebellum of bank vole's brain is presented and discussed in [9]. Density, area coverage, and distribution of cell sizes are also needed according to the input image and the required outcomes. A shape of objects can be analysed too [8, 15]. A classic approach to cell counting is the Top-Hat algorithm, but there are also other methods that are based on background removal or a general attempt for cell counting issue [10].

The SDA algorithm can act in similar way to the Top-Hat algorithm. Additionally, the threshold parameter can be taken into account to make the output less sensitive to noise. Fig. 3(a) shows an example of a sagittal section of the cerebral cortex. There is also a Top-Hat output with neighborhood radius of 12, (Fig. 3(b)) and SDA outputs for thresholds of 30 (Fig. 3(c)) and 60 (Fig. 3(d)) and a radius of 12. It can be seen that SDA outputs contain less disturbances than Top-Hat.

3.3 Hand Radiographs

Computer processing of hand radiographs is a common task in numerous studies. In most cases, the analysis requires the extraction of the contours of the fingers or the whole hand and a clear separation of the bones, particularly the phalanges [3, 2, 23]. There is no unified method to this segmentation, so approaches are typically created by authors .

For example, to obtain a separation of lines in fingers' phalanxes the Sobel gradient was used [17]. The preprocessing stage involved background removal

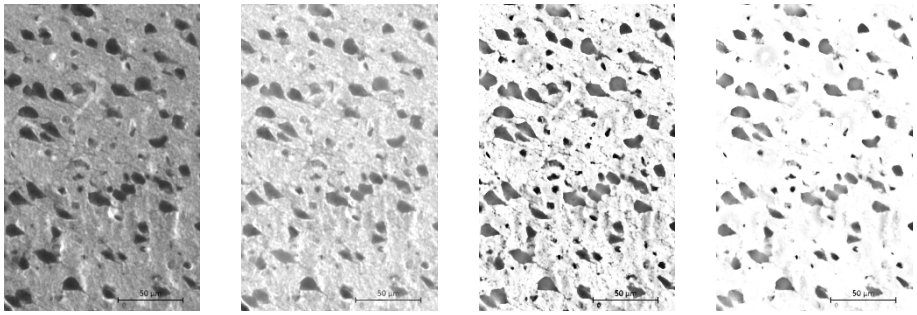

(a) original (b) Top-Hat, R=12 (c) SDA, R=12, t=30 (d) SDA, R=12, t=60

Fig. 3. An example of a sagittal section of the cerebral cortex

based on dynamic thresholding, and erosion with a 3×3 structural element was performed in order to remove all small noisy elements.

In further work [18] the authors presented a more advanced approach to preprocessing. Due to nonuniformity, background removal was performed independently for each highest peak reflecting the soft and bony structure, in relation to the average intensity of the background level. These considerations are not needed when using the SDA algorithm.

Identification of the borders of the upper and lower surfaces of phalanxes is considered in [25, 4]. The authors proposed a constructive algorithm, based on computing the path running through the borders of both surfaces. Initial border points are used to create a circle with radius equal to the distance from F to E. A special analysis checks neighboring pixels, corresponding to the surface and background. The idea of this approach is related to the SDA algorithm, which checks the content of the round (circle) neighborhood. Another approach is to adapt other algorithms [12] in order to achieve proper hand segmentation [13].

In Fig. 4, 5 the usage of the SDA algorithm is shown for a hand radiograph. Fig. 4 presents contour detection of phalanxes in which all bones are segmented correctly. Fig. 5 shows contour detection of a whole hand (size of 2712×1656) in which it can be seen that all phalanxes are separated precisely without dynamic thresholding and independent processing of selected regions of interest.

4 An Experimental Comparison of SDA and Top-Hat Algorithms

The effectiveness of algorithms can be evaluated experimentally. For this purpose, cells were counted by comparative segmentation using the standard methods of the Top Hat and Otsu algorithms. As a reference, the well-known 'rice' image was selected [21]. The size of the environment is a parameter common to both algorithms; therefore, a round neighborhood with a radius $R = 12$ was chosen. The SDA algorithm has an additional parameter: thresholding. Based

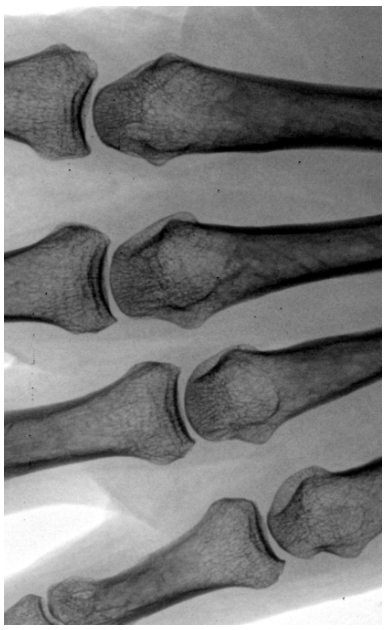

(a) original, 2712x1656, 8bit

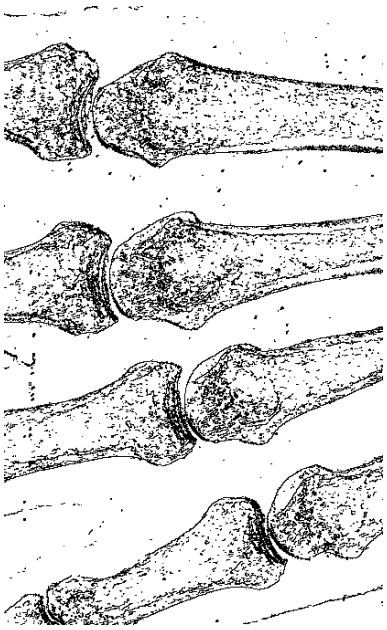

(b) Canny's algorithm output

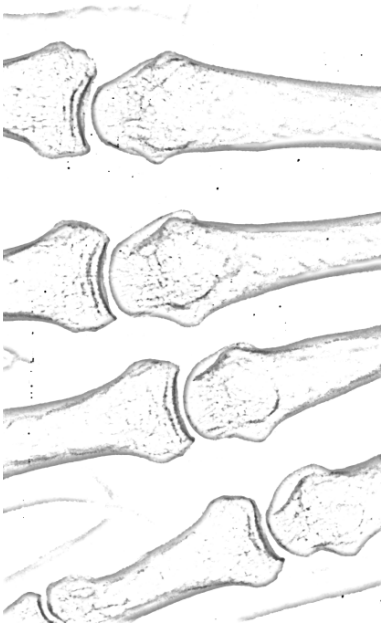

(c) SDA output, R=25, t=25

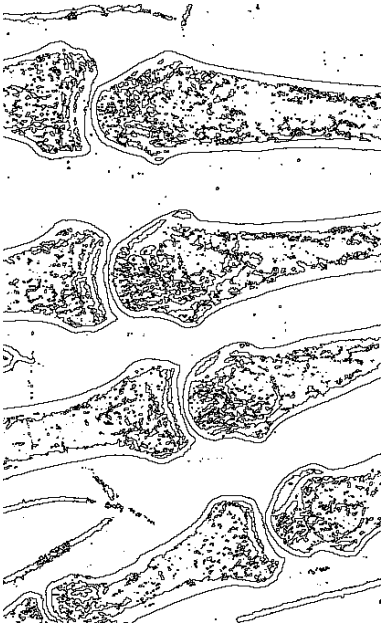

(d) SDA output after binarisation ($t_{bin} = 1$) and contour extraction

Fig. 4. A part of a hand radiograph

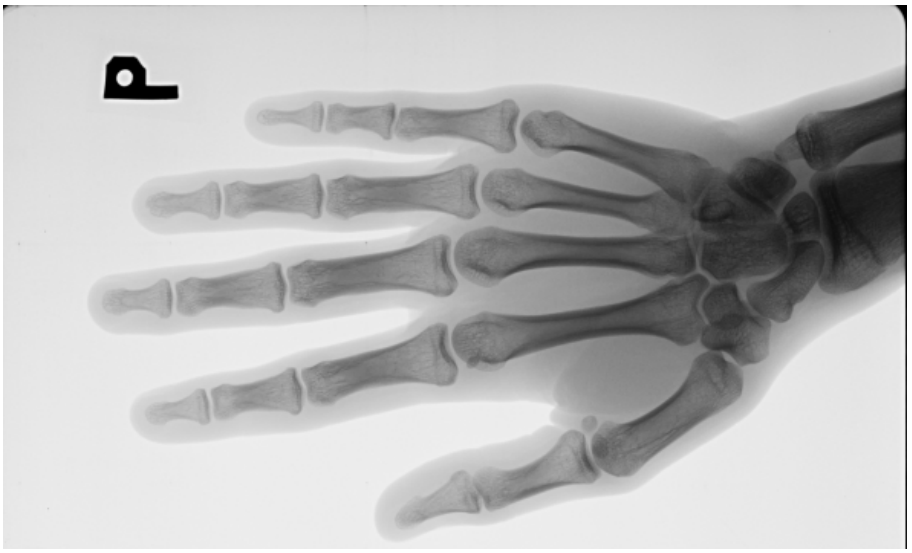

(a) original, 1425x2364, 12bit

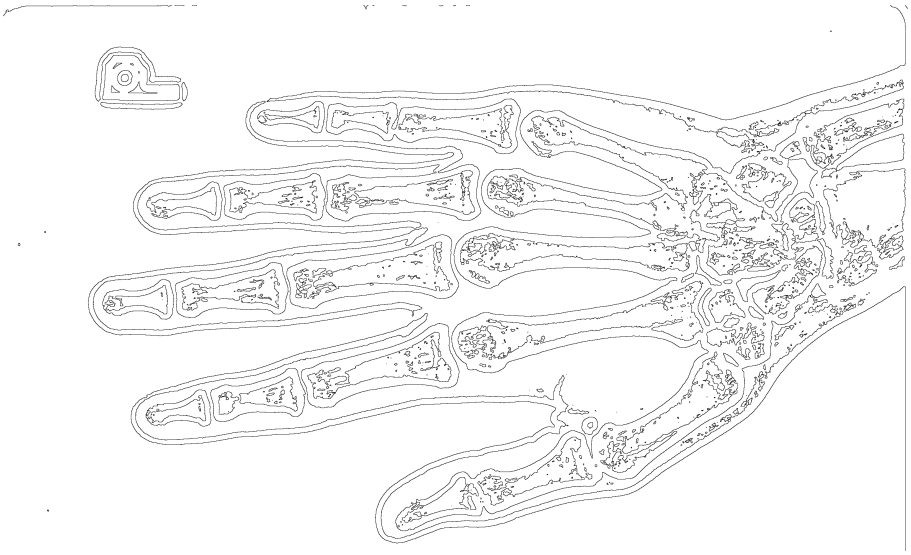

(b) SDA, R=15, t=200

Fig. 5. Full hand radiogram and its SDA output after binarisation ($t_{bin} = 1$) and contour extraction

on the selection of this parameter, overlapping results obtained with two methods were analyzed. Fig. 7(a) shows the number of points detected in one of the resulting images for a given threshold. Fig. 7(b) shows the dependence of the Dice Similarity Coefficient for a range of SDA thresholds [7]. Figure 4 shows the number of counted elements; an important parameter for cell counting.

Tests conducted on the 'rice' example image show high similarity between the SDA segmentation algorithm and the standard approach (Top-Hat, Otsu) with appropriate threshold adjustment. For the $threshold = 53$, both methods achieved the highest compliance rate, reaching a Dice Similarity Coefficient value of 0.9876. Figure 6 shows the difference between the two results. It can be argued that these differences relate mainly to single points on the edges of objects (Fig. 6(d), red and blue pixels). When the number of objects is analyzed, it can be shown that with a relatively long thresholding period (46–67), the number of detected objects is almost the same in both output images.

The advantage of the SDA algorithm over the standard approach is the ability to determine the threshold value in order to be able to choose objects with given a difference in brightness. This applies e.g. to microscopic images of nervous tissues, for which it is essential to accurately search for selected elements like glial cells.

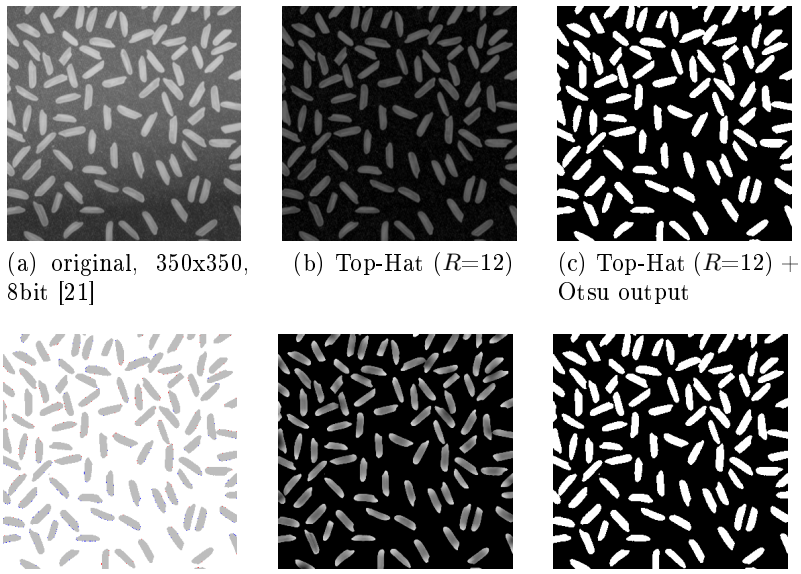

(a) original, 350x350, 8bit [21]

(b) Top-Hat (R=12)

(c) Top-Hat (R=12) + Otsu output

(d) Top-Hat and SDA differences

(e) SDA output, negated, R=12, t=53

(f) SDA output after binarisation ($t_{bin} = 1$)

Fig. 6. The image 'rice'

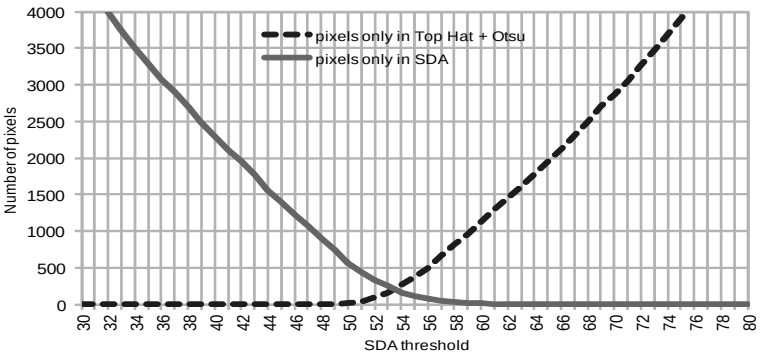

(a) Number of pixels in output test images

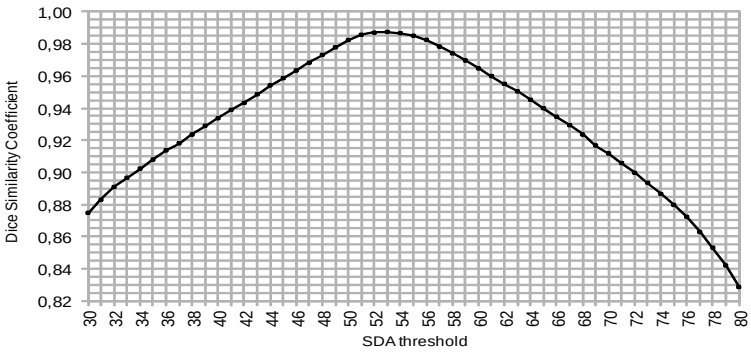

(b) Dice Similarity Coefficient

Fig. 7. A comparison of Top-Hat+Otsu and SDA outputs

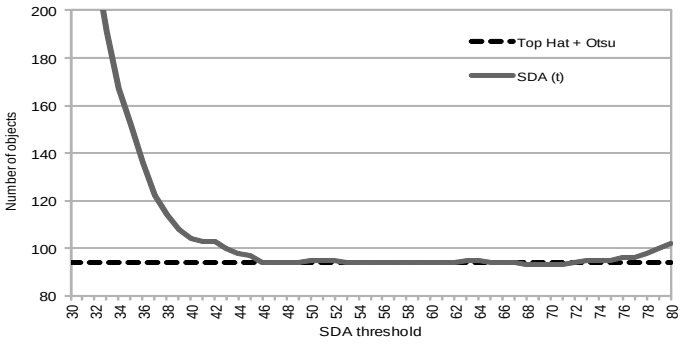

Fig. 8. Number of labeled objects in output test images

5 Summary

The SDA algorithm described in this paper seems to be notable for applications in medical image analysis. Its features are shown with various examples. The most interesting result is the distinct marking of the boundaries of corneal endothelial cells which is clear in the left half and fuzzy in the right. Also, the algorithm for cell counting tasks has been exemplified. The hand radiographs algorithm extracted the contours of phalanges reasonably well, without the need for local processing. Further research and studies should involve full testing of the proposed algorithm in detailed comparison of other well-known methods.

A sample algorithm demo is available on the site:

`home.agh.edu.pl/~pioro/sda/`

Acknowledgement. This work was financed by the AGH - University of Science and Technology, Faculty of Geology, Geophysics and Environmental Protection as a part of statutory project.

The author would like to thank to Dr J. Gronkowska–Serafin for corneal endothelium images, Dr A. Kolodziejczyk for neural tissue images, Prof. M. Korkosz and Dr M. Bielecka for hand radiographs, and Prof. R. Tadeusiewicz for consulting.

References

1. Spatial data analysis: neighbourhood and connectivity calculations. In: Ilwis 3.0 Academic Users Guide
2. Bielecka, M., Bielecki, A., Korkosz, M., Skomorowski, M., Wojciechowski, W., Zieliński, B.: Application of shape description methodology to hand radiographs interpretation. In: Computer Vision and Graphics, pp. 11–18. Springer (2010)
3. Bielecka, M., Skomorowski, M., Zieliński, B.: A fuzzy shape descriptor and inference by fuzzy relaxation with application to description of bones contours at hand radiographs. In: Adaptive and Natural Computing Algorithms, pp. 469–478. Springer (2009)
4. Bielecki, A., Korkosz, M., Wojciechowski, W., Zieliński, B.: Identifying the borders of the upper and lower metacarpophalangeal joint surfaces on hand radiographs. In: Artificial Intelligence and Soft Computing. pp. 589–596. Springer (2010)
5. Canny, J.: A computational approach to edge detection. Pattern Analysis and Machine Intelligence, IEEE Transactions on (6), 679–698 (1986)
6. Charłampowicz, K., Reska, D., Boldak, C.: Automatic segmentation of corneal endothelial cells using active contours. Advances in Computer Science Research 11, 47–60 (2014)
7. Dice, L.R.: Measures of the amount of ecologic association between species. Ecology 26(3), 297–302 (1945)
8. Jaworek-Korjakowska, J., Tadeusiewicz, R.: Design of a teledermatology system to support the consultation of dermoscopic cases using mobile technologies and cloud platform. Bio–Algorithms and Med–Systems 11(1), 53–58 (2015)

9. Kolodziejczyk, A., Ladniak, M., Piorkowski, A.: Constructing software for analysis of neuron, glial and endothelial cell numbers and density in histological nissl-stained rodent brain tissue. Journal of Medical Informatics & Technologies 23, 77–86 (2014)
10. Kuo, T., Byun, J.: ITCN (Image-based Tool for Counting Nuclei). http://www.bioimage.ucsb.edu/automatic-nuclei-counter-plug-in-for-imagej
11. Meijering, E.: Cell segmentation: 50 years down the road [life sciences]. Signal Processing Magazine, IEEE 29(5), 140–145 (2012)
12. Mikrut, Z., Bublinski, Z., Popiela-Mizera, A.: A method of linear star sections applied for object separation in ercp images. In: Image Processing, 1996. Proceedings., International Conference on. vol. 1, pp. 363–366. IEEE (1996)
13. Ogiela, M.R., Tadeusiewicz, R., Ogiela, L.: Image languages in intelligent radiological palm diagnostics. Pattern Recognition 39(11), 2157–2165 (2006)
14. Ojala, T., Pietikäinen, M., Harwood, D.: A comparative study of texture measures with classification based on featured distributions. Pattern recognition 29(1), 51–59 (1996)
15. Oszutowska-Mazurek, D., Mazurek, P., Sycz, K., Waker-Wójciuk, G.: Variogram based estimator of fractal dimension for the analysis of cell nuclei from the papanicolaou smears. In: Image Processing and Communications Challenges 4, Advances in Intelligent Systems and Computing, vol. 184, pp. 47–54. Springer (2013)
16. Otsu, N.: A threshold selection method from gray-level histograms. Automatica 11(285–296), 23–27 (1975)
17. Pietka, E., Gertych, A., Pospiech, S., Cao, F., Huang, H., Gilsanz, V.: Computer-assisted bone age assessment: Image preprocessing and epiphyseal/metaphyseal roi extraction. Medical Imaging, IEEE Transactions on 20(8), 715–729 (2001)
18. Pietka, E., Gertych, A., Pospiech-Kurkowska, S., Cao, F., Huang, H., Gilzanz, V., et al.: Computer-assisted bone age assessment: graphical user interface for image processing and comparison. Journal of Digital Imaging 17(3), 175–188 (2004)
19. Piorkowski, A., Gronkowska-Serafin, J.: Towards precise segmentation of corneal endothelial cells. In: Bioinformatics and Biomedical Engineering, Lecture Notes in Computer Science, vol. 9043, pp. 240–249 (2015)
20. Selig, B., Vermeer, K.A., Rieger, B., Hillenaar, T., Hendriks, C.L.L.: Fully automatic evaluation of the corneal endothelium from in vivo confocal microscopy. BMC Medical Imaging 15(1), 13 (2015)
21. Shoelson, B., Tannenbaum, B.: New features for high-performance image processing in matlab, http://www.mathworks.com/company/newsletters/articles/new-features-for-high-performance-image-processing-in-matlab.html
22. Smolka, B., Nurzynska, K.: Power LBP: A novel texture operator for smiling and neutral facial display classification. Procedia Computer Science 51, 1555–1564 (2015)
23. Tadeusiewicz, R., Ogiela, M.R.: Picture languages in automatic radiological palm interpretation. International Journal of Applied Mathematics and Computer Science 15(2), 305–312 (2005)
24. Tamburo, R.: An image filter for counting pixel neighbors. The Insight Journal (2011), http://hdl.handle.net/10380/3267
25. Zieliński, B., Skomorowski, M., Wojciechowski, W., Korkosz, M., Sprężak, K.: Computer aided erosions and osteophytes detection based on hand radiographs. Pattern Recognition 48(7), 2304–2317 (2015)